Charging of embedded InAs self-assembled quantum dots by space-charge techniques

W.-H. Chang, W. Y. Chen, M. C. Cheng, C. Y. Lai, and T. M. Hsu*
Department of Physics, National Central University, Chung-li, 32054 Taiwan, Republic of China

N.-T. Yeh and J.-I. Chyi
Department of Electrical Engineering, National Central University, Chung-li, 32054 Taiwan, Republic of China
(Received 9 March 2001; published 10 September 2001)

We present the results of both electrical and optical investigations of the charging of InAs self-assembled quantum dots embedded in a space-charge structure. Admittance spectroscopy was employed to study the electronic structures in quantum dots and their electron escape mechanisms. We resolved clear conductance features of different quantum-dot shells, enabling the study of electrons that escaped separately from different shells. Electron-filling modulation reflectance was used to investigate the interband transition influenced by the charging effects. Both the strengths and the energies of the interband transitions were modified in accordance with the electron occupation due to Pauli-blocking and the Coulomb-charging effects. The information acquired from these experimental observations is valuable for feasible device applications.

DOI: 10.1103/PhysRevB.64.125315 PACS number(s): 78.66.−w, 73.21.−b, 73.61.−r

I. INTRODUCTION

Self-assembled quantum dots (QD's) provide a nearly ideals zero-dimensional system for the study of charging effects on nanostructures. Due to the small dimensions of self-assembled QD's, (typically 10–100 nm in diameter), Coulomb interactions are expected to play a crucial role among the confined carriers and/or the photogenerated excitons. Charging effects on the transport properties of InAs and $In_{1-x}Ga_xAs$ QD's have been successfully demonstrated in a suitably designed tunneling structure[1,2] by the use of low-temperature capacitance measurements. This kind of tunneling structure has also been applied in the study of both intraband[3] and interband[4] transitions in charged QD's. On the other hand, space-charge techniques, such as deep-level transient spectroscopy[5,6] (DLTS) and admittance spectroscopy[7,8] have also been utilized to study various types of embedding QD systems, such as InP/GaInP,[5] InAS/GaAs,[6] and Ge/Si (Refs. 7–9) in a Schottky diode or a pn junction.

In this present work, the charging of InAs QD's embedded in a GaAs space-charge structure is investigated both electrically and optically. For the electrical characterizations, we used admittance spectroscopy to study the occupation dependence of the electron escape mechanisms. Our results could resolve clear features for different QD shells, enabling a separate investigation of the electron escape behaviors of different QD shells. On the other hand, optical characterizations were performed by using electron-filling modulation reflectance (EFR).[10] The applicability of this spectroscopic technique to the study of carrier filling and thermal distribution of a charged $In_{1-x}Ga_xAs$ QD system have been demonstrated previously.[10,11] Recently, this kind of spectroscopy has also been employed to study the Coulomb interactions in charged Ge/Si type-II QD's.[12] In this work, EFR measurements were employed to investigate the occupation dependence of the QD interband transitions. The blocking of the transition strength and the energy modification caused by occupied electrons are presented. Finally, the information acquired from admittance spectroscopy is compared with that obtained from optical spectroscopy.

II. EXPERIMENTS

The investigated sample was grown on an (001)-oriented n^+ GaAs substrate by solid-source molecular beam epitaxy. An InAs QD layer was embedded in the n-type region of a GaAs p^+-n structure, at a distance of 300 nm below the p^+-n interface. The layer structures and the corresponding band profiles are plotted in Fig. 1. The n-type doping con-

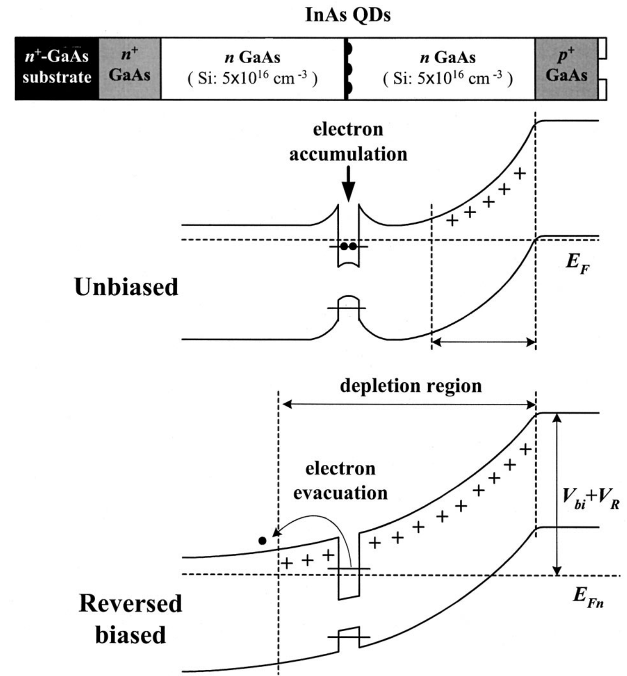

FIG. 1. The layer structure and the band profiles of the investigated p^+-n device with Fermi energy E_f under unbiased and reversed-biased conditions.

 ©2001 The American Physical Society

centration was about $5(\pm 2)\times 10^{16}$ cm^{-3}. The QD's were formed by depositing 2.7-ML InAs at 520 °C under the Stranski-Krastanow growth mode, while the growth of the other GaAs layers was maintained at 580 °C under As-stabilized conditions. According to transmission-electron-microscopy studies, the QD's had an average diameter of 20 ± 2 nm, were $\approx 3.5\pm 0.5$ nm high, with a density of 2×10^{10} cm^{-2}. In order to perform electrical measurements, the sample was processed into 500-μm square mesas. The front electrode was formed by evaporating a metal contact on the mesa top, with a 250-μm square aperture for optical access. The back contact was formed by alloying indium to the n^+-GaAs substrate. The diodes were nearly ideal, with low leakage current (≈ 1 nA) up to a reversed bias of 12 V.

The capacitance-voltage (C-V), conductance-voltage (G-V) characteristics were measured by an HP 4284A LCR meter (20 Hz–1 MHz) operated at a test signal of 10 mV. Temperature-dependent measurements were performed in a helium cryostat equipped with a temperature controller having a temperature stability better than 0.5 K. The electron-filling modulated reflectance was performed by illuminating a 1-kW tungsten-halogen lamp, combined with a 0.5 m monochromator. The modulation of electron filling in the QD levels was achieved by applying to the sample a dc bias V_{dc} with an ac voltage δV. The modulation frequency was maintained at about 200 Hz. The reflected light was collected by a cooled Ge detector. The dc components of the reflected light R were measured by an electrometer, while the modulated signals ΔR were detected using the standard lock-in technique.

III. RESULTS AND DISCUSSIONS

Figure 2 shows the C-V and the G-V characteristics measured at three selected temperatures under a test frequency of $f=1$ MHz. In each C-V profile, a pronounced capacitance plateau was observed at $V_{dc}<-2.7$ V, which originated from the electron accumulation in the InAs QD layer.[13] As the temperature is decreased down to $T=10$ K, the plateau width is suppressed, accompanying a conductance peak near the edge of the capacitance plateau ($V_{dc}=-4.5$ V). With an increasing temperature, a more extended plateau and a shift in the conductance peak toward lower biases can be observed. As the temperature is raised up to $T>130$ K, the conductance peak disappeared, and no significant changes in capacitance trace observed, except for the Debye-averaging effect, due to the increasing Debye length at the elevated temperatures.

The emergence of a conductance peak can be regarded as a fingerprint of a resonant condition for charging/discharging the QD's. When the V_{dc} is decreased from -2.7 to -6 V, the Fermi-level E_f is gradually swept from the shallower QD excited states to the deeper ground states. In this bias range, the small ac voltage of angular frequency ω ($\omega=2\pi f$) will alternatively fill and empty the QD levels. The characteristic time τ for such carrier exchanges between the QD's and the barrier is determined by the carrier emission rate e_n. When the resonant condition of $\omega\tau=1$ is satisfied, the measured conductance will exhibit a maximum. Since the time constant τ depends on both the QD confined energies and the temperature, the applied ac frequency will resonate with different QD levels as the bias and the temperature are varied.

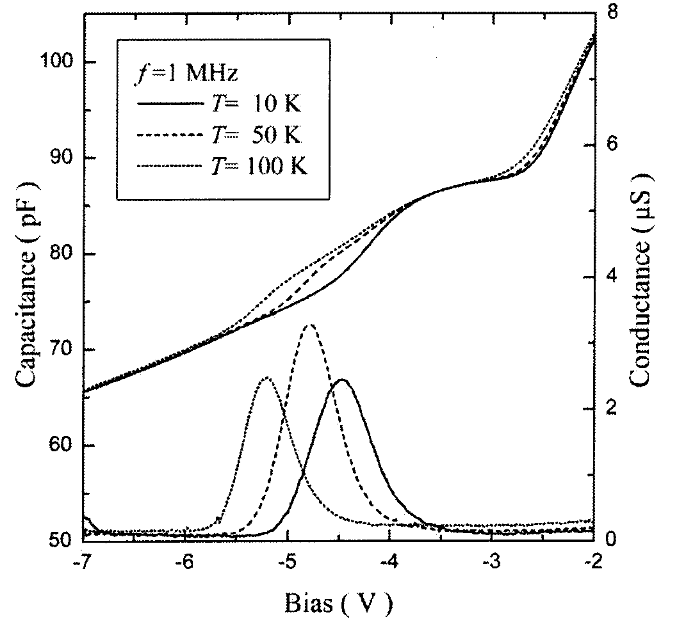

FIG. 2. The C-V and G-V characteristics measured at $T=10$ K (solid lines), 50 K (dashed lines), and 130 K (dotted lines) under a test frequency $f=1$ MHz.

In Figs. 3(a) and 3(b), the temperature evolution of the

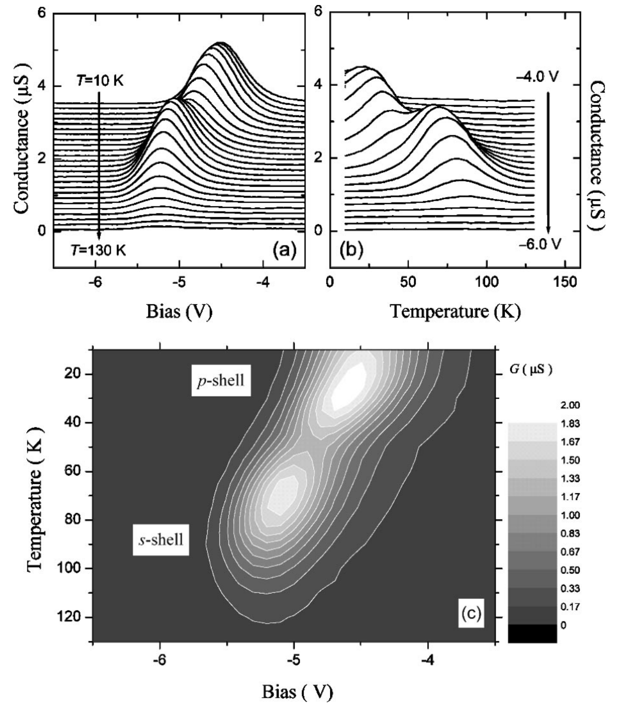

FIG. 3. (a) The temperature evolution of the 500-kHz G-V spectra, from 10 K to 130 K, with an increment of 5 K. Each curve has been offset for clarity. (b) The bias dependence of 500-kHz G-T spectra, from -4.0 to -6.0 V with an increment of 0.1 V. Each curve has also been offset for clarity. (c) Contour plot of the above conductance peaks.

conductance spectra is displayed in more detail. The most interesting feature is that the amplitude of the conductance maximum G_{max} also varies in accordance with the applied bias and the temperature. As can be clearly seen in the contour plot displayed in Fig. 3(c), these conductance spectra exhibit two maxima: one near $V_{dc} \approx -4.6$ V for $T \approx 30$ K, while the other one appears near $V_{dc} \approx -5.2$ V for $T \approx 70$ K. Since the G_{max} is proportional to the number of electrons being exchanged between the dots and the barrier, the observed double-peak feature can be attributed to the charging of different QD shells. In Fig. 3(c), the G_{max} at the lower bias (-5.2 V) is ascribed to the charging of QD ground state (*s* shell), while the higher-bias one (-4.6 V) is related to the first QD excited state (*p* shell). It is worth noting that the capacitance plateau in Fig. 2 appears in the bias range of $-5.6 \text{ V} < V_{dc} < -2.7$ V, while the conductance features are only observed in the range of $-5.6 \text{ V} < V_{dc} < -4$ V. This implies that the electrons can be further charged into the QD *d* shell and/or the wetting layer when the V_{dc} is increased to -2.7 V. However, the emission rate for these higher-energy states may be too fast to be resolved with the available frequency and temperature ranges of our experimental setups.

The double-peak feature appearing in the *G-T* spectra enables us to extract the thermal activation behaviors of electrons in different QD states. To analyze the temperature- and frequency-dependent QD conductance $G(\omega,T)$, a detailed knowledge of the ac response of carriers being exchanged between the dots and the barrier is required. In the Appendix, we have derived $G(\omega,T)$ based on the Shockley-Read-Hall dynamics.[14] Since the thermionic emission rate depends exponentially on both the activation energy E_A and the temperature,[15] i.e., $e_n(T) = \gamma\sigma T^2 \exp(-E_A/k_B T)$, where γ is a temperature-independent factor, σ is the captured cross section, and k_B is the Boltzmann constant. At a given bias, when the *G-T* spectra reach a maximum at a temperature T_{max} the emission rate can be approximated by $e_n(T_{max}) \approx \omega/2$. Thus, by measuring the *G-T* spectra at different V_{dc} and ω, the activation energies can be deduced from the Arrhenius plot of e_n/T_{max}^2 vs $1/T_{max}$. These results are displayed in Fig. 4. For each V_{dc}, the *G-T* spectra were taken at six measurement frequencies ranging from 50 kHz to 1 MHz. In this figure, the Arrhenius plots acquired from the *s*-shell features are almost linear, having linear correlation coefficients larger than 0.9995. However, we note that the data obtained from the *p*-shell features are not linear, especially when $V_{dc} = -4.3$ V. This behavior can be attributed to the direct tunneling effect. Since the tunneling process is temperature independent, the Arrhenius plot will significantly deviate from a linear relation when the (field-assisted) tunneling process is involved. Taking the direct tunneling rate e_t into account, the total emission rate e_n^{total} can be expressed as

$$e_n^{\text{total}} = e_t + \gamma\sigma T^2 \exp(-E_A/k_B T). \tag{1}$$

In this equation, the values of E_A, e_t, and σ were treated as fitting parameters. Figure 5(a) shows the deduced activation energy E_A, as a function of the bias voltage V_{dc}. For the QD

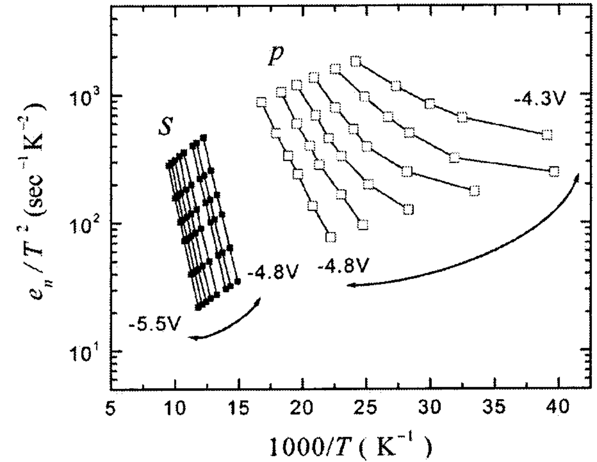

FIG. 4. The Arrhenius plots obtained from *G-T* spectra with different bias voltages, taken at frequencies ranging from 50 kHz to 1 MHz. The investigated bias ranged from -5.5 to -4.3 V, with an increment of 0.1 V. Due to the double peaks that appeared in the *G-T* spectra (see Fig. 3), both the *s*- and *p*-shell features are included for $V_{dc} = -4.8$ V.

s shell, the deduced E_A values fall in the range of 82–95 meV, and the fitted e_t values are virtually zero. The obtained *p*-shell E_A's are in the range of 14–41 meV but are less accurate then the *s*-shell ones due to the involvement of the

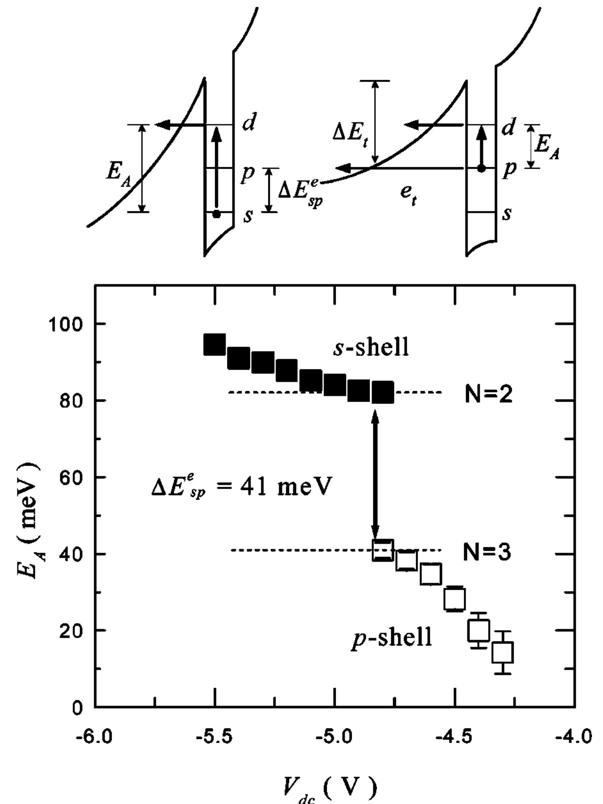

FIG. 5. (a) Activation energies for the QD *s* shell and *p* shell, as a function of bias deduced from the Arrhenius plot shown in Fig. 4. (b) Schematic diagrams for the electron escape mechanism described in the text.

direct tunneling effect. The fitted e_t values, for direct tunneling from the p shell, ranged from 1.9×10^4 to $2.2\times10^5\,\mathrm{sec}^{-1}$, as the bias was increased from -4.8 to -4.3 V. Between the s and the p shells, we observed an energy splitting of $\Delta E_{A,sp}\approx41$ meV at $V_{dc}=-4.8$ V. This value can be considered as the E_A difference between the second electron in the s shell ($N=2$) and the first electron in the p shell ($N=3$). The fitted e_t can be further utilized to estimate the tunneling barrier ΔE_t by the Wentzel-Kramers-Brillouin (WKB) method.[16] For example, at $V_{dc}=-4.8$ V, we obtained a tunneling barrier of $\Delta E_t\approx216$ meV for the first p-shell electron.

According to the obtained E_A's and the estimated ΔE_t, the electron escape mechanism can be summarized as in Fig. 5(b). It is clear that the QD electrons are not directly thermally activated into the GaAs barrier, since the electron ground state of our dot may be ~250 meV below the GaAs barrier, according to the theoretical calculation of InAs QD with a similar size.[17] Thus, the obtained activation energies suggest a two-step activation process: thermal activation to the QD excited state and then subsequent tunneling into the GaAs, by the assistance of electric field. This can be further confirmed by the estimated ground-state confinement $\Delta E_t+\Delta E_{A,sp}\approx257$ meV, which agrees very well with the theoretical prediction. This two-stage process has been proposed by Kapteyn *et al.*,[6] based on DLTS measurements of a similar InAs QD system. They reported a value of $E_A=94\pm5$ meV, and attributed this value to the energy difference between the QD s and p shells. However, in our experiment, we observed ≈41 meV as where the s-p splitting in the activation energy occurs. The s- and p-shell electrons are more likely to be thermally activated into higher-excited state (e.g., d shell), since the deduced E_A's for the s shell are nearly twice as large as those of the p shell.

The charging of the InAs QD's was also optically investigated by EFR measurements. The EFR was performed by applying a bias modulated between a lower-bias level V_L and a higher level V_H. The V_H was kept at 0 V as a referent level, whereas the V_L was varied in the present investigation. As implied by the measured C-V characteristics, the QD's were charged at least up to the d shell under an unbiased condition. Thus, adapting $V_H=0$ V as a reference is very suitable, since the the interband transitions for those occupied states will be blocked. In Fig. 6, the V_L-dependent EFR spectra are displayed. For the case of $V_L=-6.6$ V, all the QD states are unoccupied. We observe three interband transitions (labeled as s-s, p-p, and d-d), which are the transitions between different electron and hole shells of *neutral* QD's. When the bias was increased up to $V_L>-5.8$ V, the s-s transition intensity decreased gradually, being fully blocked when $V_L>-5.0$ V. This indicates that the electrons were gradually charged into the s shell in this bias range, which is consist with the conductance measurement displayed in Fig. 3.

Similarly, the p-p transition was gradually blocked when the electrons were charged into the p shell ($V_L>-4.8$ V). In addition to the blocking of interband transitions, substantial energy shifts, in accordance with the electron occupations, were also observed. This behavior is illustrated in Fig. 7. For $V_L<-5.8$ V, slight blueshifts were observed with the increasing V_L in both the s-s and the p-p transition energies. Since the QD's are neutral in this bias range, this blueshift can be attributed to the decreasing electric field across the QD's, i.e., the quantum-confined Stark effect (QCSE).[18] The field dependence of this energy shift is very similar to our previously reported Stark shift in similar InAs dots.[19] In the range of $-5.8\ \mathrm{V}<V_L<-4.8$ V, the p-p transition shows a remarkable redshift of 10 ± 2 meV. At $V_L=-4.8$ V, the doubly degenerated s shell was fully occupied. The optically excited electron-hole (e-h) pair in the QD p-p shells will

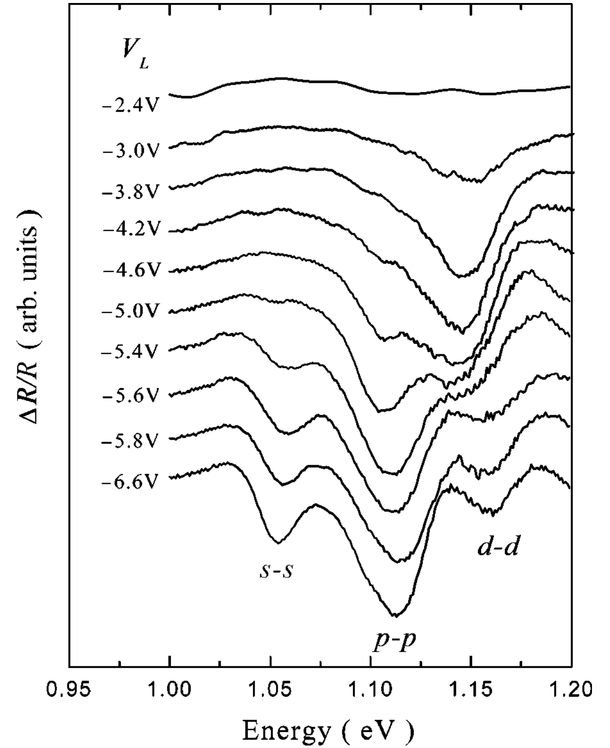

FIG. 6. The EFR spectra obtained by modulating the bias voltage between a constant $V_H=0$ V and varied V_L.

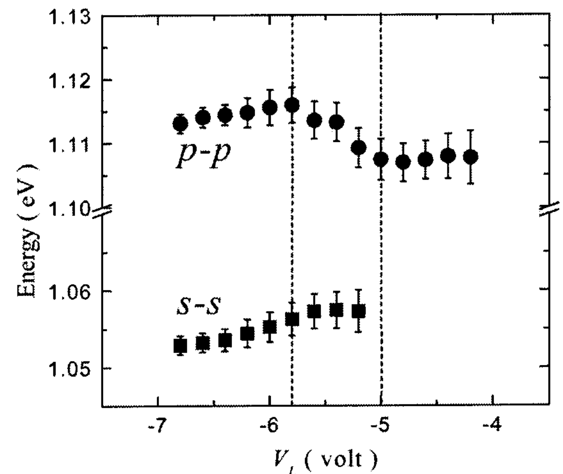

FIG. 7. The bias dependence of s-s and p-p transition energies obtained from the EFR spectra shown in Fig. 6.

TABLE I. The Coulomb interaction and the exchange energy, between carriers in QD s and p shells, calculated by the perturbation model. The subindexes i and j represent QD s or p shells, i.e., E_{ij}^{ee} is the ee Coulomb energy between i-shell and j-shell electrons, E_{ij}^{eh} is the eh Coulomb energy between i-shell electron and j-shell hole, and E_{ij}^{x} is the exchange energy between the i-shell and j-shell electrons.

i,j	E_{ij}^{ee} (meV)	E_{ij}^{eh} (meV)	E_{ij}^{x} (meV)
s,s	22.3	26.1	
s,p	16.7	22.1	5.6
p,p	15.3	17.3	4.2

experience additional Coulomb interactions due to these two occupied s electrons, forming negatively charged p-p excitons. If the exchange interaction between electrons was further included, the net energy shift in p-p transition, $\Delta E_{p\text{-}p}$, due to the doubly occupied s electrons is given by[4]

$$\Delta E_{p\text{-}p}=2E_{sp}^{ee}-2E_{sp}^{eh}-E_{sp}^{x}, \qquad (2)$$

where E_{sp}^{ee} is the repulsive Coulomb energy between the s and p electrons, E_{sp}^{eh} is the attractive Coulomb energy between the s electron and the p hole, and E_{sp}^{x} is the exchange energy between the optically excited p electron and one of the loaded s electrons (with the same spin orientation). As a first approximation, if the energies of the electron-electron (ee) repulsion and eh attraction are roughly the same, i.e., $E_{sp}^{ee}\approx E_{sp}^{eh}$, the observed $\Delta E_{p\text{-}p}=-(10\pm 2)$ meV may be close to the exchange energy E_{sp}^{x}. However, this value should be considered as an upper limit, since the eh attractive energy E_{sp}^{eh} is commonly slightly larger than the ee repulsive energy E_{sp}^{ee} due to the different effective mass and confinement length between the electron and the hole.

To further compare our experimental results with theoretical predictions, we adapt the perturbation model proposed by Warburton *et al.*[20] to estimate the Coulomb interaction and exchange energies,[21] which are summarized in Table I. From these interaction energies and Eq. (2), we obtain a somewhat larger energy shift of $\Delta E_{pp}=-16.2$ meV, compared with our experimental observation. In fact, we have also slightly changed the input parameters in the model calculations, but the predicted redshift is still more or less larger than the observed $-(10\pm 2)$ meV. We therefore tend to believe that this discrepancy very likely arises from the electric-field effect. In the space-charge structure, the QD's are subjected to a relatively strong electric field in the investigated bias range. In general, the effect of electric field on the ee interaction is negligible, since they possess charge of the same sign. However, the electric-field effect on the eh interaction will be relatively stronger, since the electric field tends to spatially separate the electron and the hole along the growth direction, and hence reducing the eh attractive energy E_{sp}^{eh}. Thus, according to Eq. (2), the net redshift of $\Delta E_{p\text{-}p}$ is expected to be smaller. For the s-s transition, negatively charged exciton is also formed when another s electron is loaded. This situation refers to the bias range, -5.8 V $<V_{dc}\leqslant -5.0$ V. Theoretically, the energy shift in the s-s transition, due to the occupied s electron is given by $\Delta E_{s\text{-}s}=E_{ss}^{ee}-E_{ss}^{eh}$. From Table I, we estimate an energy shift of $\Delta E_{s\text{-}s}=-3.8$ meV. However, the predicted redshift is not resolved in Fig. 7. It is very likely that the overall blueshift, caused by the QCSE, smeared the relatively smaller redshift induced by the loaded s electron. Moreover, the electric field may reduce the eh interaction E_{ss}^{eh} somewhat, further weakening the net redshift in the transition energy of a charged s-s exciton.

We now intend to relate information acquired by EFR spectroscopy to the bias-dependent activation energy deduced from admittance spectroscopy. For type-II Ge/Si QD system, Zhang *et al.*[7] have reported discrete shell structures that comprise clear ee Coulomb charging features in bias-dependent E_A spectra, determined by their admittance measurements. In our InAs QD system, according to Table I, the estimated ee Coulomb energies are $\approx 15-22$ meV. However in Fig 5, we cannot resolve any clear features that can be related to the above mentioned Coulomb-charging energies. The only discrete feature observed is the activation-energy splitting of $\Delta E_{A,sp}\approx 41$ meV at $V_{dc}=-4.8$ V. This splitting can be reasonably regarded as the energy difference between the second s electron ($N=2$) and the first p electron ($N=3$). We wish to further state that the measured $\Delta E_{A,sp}$ does not involve the Coulomb charging energy. This can be realized by comparing the $\Delta E_{A,sp}$ to the interband energy splitting ΔE_{sp}, between the s-s and the p-p transitions. In Fig. 6, we observe an interband splitting of $\Delta E_{sp}\approx 62\pm 2$ meV in unoccupied QD's ($V_L<-5.8$ V). This interband energy splitting can be divided into electron-level (ΔE_{sp}^{e}) and hole-level splitting (ΔE_{sp}^{h}), i.e., $\Delta E_{sp}=\Delta E_{sp}^{e}+\Delta E_{sp}^{h}$. Since the hole's effective mass is heavier than the electron's, the interband splitting is dominated by electron-level splitting, i.e., $\Delta E_{sp}^{e}>\Delta E_{sp}^{h}$. However, if the observed $\Delta E_{A,sp}$ also involves the e-e Coulomb energy E_{sp}^{ee}, it will lead to an unreasonably small electron-level splitting of $\Delta E_{sp}^{e}=\Delta E_{A,sp}-E_{sp}^{ee}=24.3$ meV. Therefore, we believe that the measured $\Delta E_{A,sp}$ does not involve the Coulomb-charging energy between the s and the p electrons. On the other hand, if we further assume an electron-hole splitting ratio of $\Delta E_{sp}^{e}:\Delta E_{sp}^{h}\approx 2:1$, the electron-level splitting may be roughly $\Delta E_{sp}^{e}\approx 41.3$ meV, which agrees very well with the measured $\Delta E_{A,sp}\approx 41$ meV.

The absence of Coulomb-charging features in our E_A spectrum can be realized from the two-step escape mechanism, as described in Fig. 5(b). Due to the two-step escape process, electrons at lower-energy states are thermally excited to the QD excited states. The energy required for thermally exciting the QD electrons to a higher-excited state is occupation independent, which has been demonstrated in our previous paper.[11] This situation is also similar to the infrared measurement reported by Fricke *et al.*,[3] in which the intraband absorption clearly shows an occupation-independent behavior. Therefore, whenever an indirect activation takes place in a QD system, it is impossible to extract the shell structures of the Coulomb-charging energies by measuring the corresponding activation energies.

IV. CONCLUSIONS

In summary, we have presented both electrical and optical investigations of the charging of InAs quantum dots embedded in a space-charge structure by the use of admittance spectroscopy and electron-filling modulation reflectance. We clearly resolved features of quantum-dot s and p shells from the admittance spectroscopy, enabling us to study electron emission mechanisms from different shells. In the optical investigations, the interband transitions demonstrated clear Pauli-blocking and Coulomb charging effects, in accordance with the electron occupation in the dots, controlled by the bias voltage. The information acquired from these experimental observations is valuable for feasible device applications. For instance, the Pauli-blocking effects exhibited in quantum dots can be utilized in a high-speed QD optical modulator, which can modulate a QD laser by integrating it in the same chip. On the other hand, the presented structure can also be applied in a charge-tunable infrared detector, providing a tunable spectral range and responsibility. However, to increase the on/off ratio of the proposed modulator, or the responsibility of the proposed infrared detector, one could increase the active QD layers, and incorporating them into waveguide structures if necessary.

ACKNOWLEDGMENTS

The authors would like to thank the Optical Center of the National Central University for the use of their MBE system. This work was supported in part by the National Science Council of the Republic of China under Grant No. NSC89-2112-M-008-063.

APPENDIX: FREQUENCY AND TEMPERATURE DEPENDENCE OF QUANTUM-DOT CONDUCTANCE

Considering the case of InAs QD's in n-type GaAs barrier, the transient response of the electron population n_{dot} of a QD level, satisfies the following differential equation:

$$\frac{dn_{\mathrm{dot}}}{dt} = -e_n n_{\mathrm{dot}} + c_n(N_{\mathrm{dot}} - n_{\mathrm{dot}}),$$

where N_{dot} and n_{dot} are the number of quantum states and the electron population of the QD's; e_n is the electron emission rate and $c_n = \sigma \nu n_0$ is the electron capture rate, in which σ is the capture cross section, ν is the thermal velocity, and n_0 is the equilibrium electron concentration in the GaAs barrier. Under steady-state conditions, i.e., $dn_{\mathrm{dot}}/dt = 0$, we obtain

$$e_n f_{eq} = \sigma \nu n_0 (1 - f_{eq}),$$

where f_{eq} is the equilibrium occupation fraction, which is given by

$$f_{eq} = \frac{n^0_{\mathrm{dot}}}{N_{\mathrm{dot}}} = \frac{1}{N_{dot}} \int \frac{D(E_i, E)}{1 + \exp[-(E - E_f)/k_B T]} dE,$$

where n^0_{dot} is the equilibrium electron population of the QD's, $D(E_i, E)$ is the QD density of state, in which E_i is the energy of QD level, and E_f is the Fermi level. For a small perturbation at a given angular frequency ω, the change of population δn_{dot}, from the equilibrium value n^0_{dot} is given to first order by

$$\frac{d\,\delta n_{\mathrm{dot}}}{dt} = j\omega\,\delta n_{\mathrm{dot}} = -(e_n + \sigma \nu n_0)\,\delta n_{\mathrm{dot}} + \sigma \nu N_{\mathrm{dot}}(1 - f_{eq})\,\delta n_0,$$

where $j = \sqrt{-1}$. Because of $n_0 = N_C \exp[-(E_C - E_f)/k_B T]$, we obtain $\delta n_0 = n_0(q\,\delta\phi/k_B T)$, where N_C and E_C are the effective density of states and the conduction band edge of the GaAs barrier, q is the electron charge, and $\delta\phi$ represents the potential difference of $(E_C - E_f)/q$ at the QD layer caused by the applied ac bias. Therefore, we get

$$\delta n_{\mathrm{dot}} = N_{\mathrm{dot}} \left(\frac{q\,\delta\phi}{k_B T} \right) \left[\frac{f_{eq}(1 - f_{eq})}{1 + j\omega(1 - f_{eq})/e_n} \right].$$

For a device of area S, the applied ac voltage δV will alternately fill and empty the QD levels, inducing an ac current $\delta I = Sq(d\,\delta n_{\mathrm{dot}}/dt)$. The QD conductance G can be obtained by taking the real part of $\delta I/\delta V$. Finally, if we define the time constant, $\tau = (1 - f_{eq})/e_n$, the QD conductance is given by

$$G(\omega, T) = \alpha \frac{f_{eq}(1 - f_{eq})}{k_B T} \left(\frac{\omega^2 \tau}{1 + \omega^2 \tau^2} \right), \qquad \text{(A1)}$$

where $\alpha = Sq^2 N_{\mathrm{dot}} \beta$ is a temperature-independent factor, in which $\beta \equiv (\delta\phi/\delta V)$. In this equation, the function $f_{eq}(1 - f_{eq})$ exhibits a peak when $f_{eq} = 1/2$, (i.e., $E_f = E_i$), and then drops exponentially to zero when E_f deviates from E_i. Moreover, the frequency-dependent factor $\omega^2\tau/(1 + \omega^2\tau^2)$ has a maximum value of 1/2 when $\omega\tau = 1$. As a result, when the condition of

$$\omega = 1/\tau = 2e_n \qquad \text{(A2)}$$

is fulfilled, the QD conductance will reach a maximum G_{max}.

*Electronic address: tmhsu@phy.ncu.edu.tw

[1] H. Drexler, D. Leonard, W. Hansen, J.P. Kotthaus, and P.M. Petroff, Phys. Rev. Lett. **73**, 2252 (1994).

[2] G. Medeiros-Ribeiro, D. Leonard, and P.M. Petroff, Appl. Phys. Lett. **66**, 1767 (1995).

[3] M. Fricke, A. Lorke, J.P. Kotthaus, G. Medeiros-Ribeiro, and P.M. Petroff, Europhys. Lett. **36**, 197 (1996).

[4] R.J. Warburton, C.S. Dürr, K. Karrai, J.P. Kotthaus, G. Medeiros-Ribeiro, and P.M. Petroff, Phys. Rev. Lett. **79**, 5282 (1997).

[5] S. Anand, N. Carlsson, M.E. Pistol, L. Samuelson, and W. Seifert, Appl. Phys. Lett. **67**, 3016 (1995).

[6] C.M.A. Kapteyn, F. Heinrichsdorff, O. Stier, R. Heitz, M. Grundmann, N.D. Zakharov, D. Bimberg, and P. Werner, Phys. Rev. B **60**, 14 265 (1999).

[7] S.K. Zhang, H.J. Zhu, F. Lu, Z.M. Jiang, and Xun Wang, Phys. Rev. Lett. **80**, 3340 (1998).

[8] C. Miesner, T. Asperger, K. Brunner, and G. Abstreiter, Appl. Phys. Lett. **77**, 2704 (2000).
[9] C.M.A. Kapteyn, M. Lion, R. Heitz, D. Bimberg, C. Miesner, T. Asperger, K. Brunner, and G. Abstreiter, Appl. Phys. Lett. **77**, 4169 (2000).
[10] T.M. Hsu, W.-H. Chang, K.F. Tsai, J.-I. Chyi, N.T. Yeh, and T.E. Nee, Phys. Rev. B **60**, R2189 (1999).
[11] W.-H. Chang, T.M. Hsu, N.T. Yeh, and J.-I. Chyi, Phys. Rev. B **62**, 13 040 (2000).
[12] A.I. Yakimov, N.P. Stepina, A.V. Dvurechenskii, A.I. Nikiforov, and A.V. Nenashev, Phys. Rev. B **63**, 045312 (2001).
[13] P.N. Brounkov, A. Polimeni, S.T. Stoddart, M. Henini, L. Eaves, P.C. Main, A.R. Kovsh, Yu.G. Musikhin, and S.G. Konnikov, Appl. Phys. Lett. **73**, 1092 (1998).
[14] The method of analyzing the ac response of carrier being exchanged between the dots and the barrier is similar to those commonly employed for the defect states in semiconductors, see for example, J. Bourgoin and M. Lannoo, *Point Defects in Semiconductors II* (Springer-Verlag, Berlin, 1983).
[15] See, for example, D.V. Lang, J. Appl. Phys. **45**, 3023 (1974).
[16] X. Letartre, D. Stiévenard, M. Lannoo, and E. Barbier, J. Appl. Phys. **69**, 7336 (1991).
[17] O. Stier, M. Grundmann, and D. Bimberg, Phys. Rev. B **59**, 5688 (1999).
[18] P.W. Fry, I.E. Itskevich, D.J. Mowbray, M.S. Skolnick, J.J. Finley, J.A. Barker, E.P. O'Reilly, L.R. Wilson, I.A. Larkin, P.A. Maksym, M. Hopkinson, M. Al-Khafaji, J.P.R. David, A.G. Cullis, G. Hill, and J.C. Clark, Phys. Rev. Lett. **84**, 733 (2000).
[19] T.M. Hsu, W.-H. Chang, C.C. Huang, N.T. Yeh, and J.-I. Chyi, Appl. Phys. Lett. **78**, 1760 (2001).
[20] R.J. Warburton, B.T. Miller, C.S. Dürr, C. Bödefeld, K. Karrai, J.P. Kotthaus, G. Medeiros-Ribeiro, P.M. Petroff, and S. Huant, Phys. Rev. B **58**, 16 221 (1998).
[21] To estimate the Coulomb energies and the exchange energies between the carriers confined in a quantum dot with parabolic potential, we need to know the effective mass m_e^* (m_h^*) and the effective confinement length l_e (l_h) of the electron (hole). The values of l_e (l_h) can be deduced from the electron(hole)-level splitting $\hbar\omega_e$ ($\hbar\omega_h$) of the parabolic potential. In our calculation, we assume an electron-hole level-splitting ratio of $\hbar\omega_e:\hbar\omega_h=2:1$, then we obtain $\hbar\omega_e=41.3$ meV and $\hbar\omega_h=20.7$ meV, based on the measured interband energy splitting of $\Delta E_{sp}=62$ meV. The effective mass values, m_e^* and m_h^*, were adapted from Ref. 20.